J. Dairy Sci. 109:1784–1799
https://doi.org/10.3168/jds.2025-27278

Genomic regions associated with blood metabolites and subclinical ketosis in early-lactation Holstein cows

S. Magro,[1] A. Costa,[2]* J. Vegni,[2] J. B. C. H. M. van Kaam,[3] R. Finocchiaro,[3] M. Marusi,[3] M. Cassandro,[1,3] and M. De Marchi[1]
[1]Department of Agronomy, Food, Natural Resources, Animals and Environment, University of Padova, 35020 Legnaro, Italy
[2]Department of Veterinary Medical Sciences, Alma Mater Studiorum University of Bologna, 40064 Ozzano dell'Emilia, Italy
[3]Associazione Nazionale Allevatori della Razza Frisona, Bruna e Jersey Italiana, 26100 Cremona, Italy

ABSTRACT

Modern dairy cattle populations have been intensively selected for high milk production; therefore, cows experience significant metabolic stress after calving and during the transition period. Breeding strategies aimed at making cows more robust and resistant to diseases without compromising milk productivity exist and have been implemented in some countries. Whereas genomic investigations have been conducted on both clinical and subclinical forms of ketosis, few studies have focused on measurable features reflecting metabolic processes, such as the blood concentrations of BHB and nonesterified fatty acids (NEFA) and urea, an indicator of nitrogen metabolism. A better understanding of the coding genes and polygenic nature of blood metabolites is advisable for genomic selection and evaluation. Therefore, this study aimed to identify genomic regions associated with major hematic biomarkers of ketosis predicted from mid-infrared milk spectra in the Italian Holstein population. A single-step GWAS was performed using predicted blood phenotypes collected from 6,190 clinically healthy Holstein cows from 5 to 35 DIM, reared in 374 herds, and genotyped with arrays of different SNP density. The analyzed traits included: BHB (log-transformed), NEFA (log-transformed), urea concentration (mmol/L), and subclinical ketosis (SCK), which was identified when BHB was ≥1.20 mmol/L. Specifically, 5.51% of cows were identified as being at risk of SCK. After imputation and conventional quality control, 64,202 markers located in the autosomes were used for the association study. The genomic h^2 was generally low (<0.11) for all the traits investigated. Signals of BHB were scattered across several locations (BTA2, 4, 6, 7, 18, 21, 22, 25, and 28) in regions related to metabolic processes and immune system function and response. In contrast, the significant SNP for SCK were mainly concentrated in BTA1, 5, 11, and 15, confirming the combined action of multiple genes on health-related phenotypes and suggesting that the genetic control of SCK is more restricted to specific chromosomal regions than that of blood biomarker concentration. For traits such as NEFA and urea, the number of significant signals was lower, and they were mainly related to lipid metabolism. Although the results should be interpreted with caution and validated in future research, our findings provide novel insights into the genetic and molecular mechanisms underlying negative energy balance and SCK in Holstein cows, offering potential targets for future functional studies and genetic improvement strategies.
Key words: GWAS, polygenic trait, metabolic disorder, transition cow, ketosis

INTRODUCTION

Subclinical ketosis (**SCK**) is a costly disorder in dairy cattle (Rasmussen et al., 2024) because it is associated with an increased risk of health issues, exposing cows to other diseases and metabolic disorders. Regardless of whether they are clinical or subclinical, negative energy balance (**NEB**) and associated conditions are responsible for compromised reproductive performance, changes in milk production and quality, and, therefore, a high likelihood of culling (Raboisson et al., 2014). In particular, Steeneveld et al. (2020) reported that the average cost of a single case of SCK was €150 (range €18–€422) with contributions for milk loss (62%), treatment (13%), reproduction (12%), culling (7%), and other diseases (6%), respectively.

Both mild NEB and SCK can be identified through high blood ketone body concentrations without the presence of clinical signs. Specifically, it is characterized by a blood BHB concentration greater than 1.20 mmol/L during early lactation (MacArt et al., 2012). However, both elevated BHB and nonesterified fatty

Received July 21, 2025.
Accepted November 3, 2025.
*Corresponding author: angela.costa2@unibo.it

The list of standard abbreviations for JDS is available at adsa.org/jds-abbreviations-25. Nonstandard abbreviations are available in the Notes.

Table 1. Descriptive statistics[1] and genomic h^2 of cows' blood traits analyzed

Trait	Mean (SD)	Range	h^2 (SE)
Log_{10}BHB	−0.20 (0.18)	−0.76–0.61	0.11 (0.02)
BHB, mmol/L	0.69 (0.32)	0.17–4.07	0.10 (0.02)
Log_{10}NEFA	−0.53 (0.44)	−3.42–0.77	0.03 (0.01)
NEFA, mmol/L	0.49 (0.58)	0.00–5.87	0.03 (0.01)
Urea, mmol/L	2.63 (1.57)	0.12–8.11	0.06 (0.02)
SCK[2]	0	1	0.03 (0.01)

[1]For BHB and NEFA, values corresponded to back-transformed data from log_{10} scale.
[2]Healthy (5,849 cows): BHB <1.20 mmol/L. Affected (341 cows): BHB ≥1.20 mmol/L.

acids (**NEFA**) are commonly used as markers of hyperketonemia (Benedet et al., 2019) and SCK (Ospina et al., 2010). In particular, BHB concentrations between 1.2 and 2.9 mmol/L suggest SCK, whereas concentrations ≥3.0 mmol/L suggest clinical form (Benedet et al., 2019). Modern dairy cattle populations have been intensively selected for high milk production but experience significant metabolic stress during the transition period. This selective pressure has led to side effects, such as a higher incidence of reproductive health issues and production-related diseases (Costa et al., 2024). Suthar et al. (2013) considered 5,884 dairy cows, mainly of the Holstein breed, reared in 528 herds, and reported an average prevalence of SCK of 21.8% across 10 different countries, with the highest percentage recorded in Italy (36.6%). Nowadays, there is a global interest in breeding more robust dairy cattle with greater disease resistance. Despite the low h^2 (<0.17) found for both clinical ketosis (Oliveira-Junior et al., 2021) and milk (Lee et al., 2016) and blood BHB concentrations (Belay et al., 2017; Benedet et al., 2020; Magro et al., 2025), susceptibility to metabolic disorders is still under genetic control and, to a certain extent, could be reduced through genetic selection (Pryce et al., 2016).

Based on current knowledge, it can be reasonably assumed that there are undisclosed associations between fitness/health traits and productive performance and likely antagonism between genomic regions playing a role in phenotypes. Kroezen et al. (2018) reported that genes encoding proteins involved in metabolic processes—including the synthesis and degradation of fatty acids and ketone bodies, gluconeogenesis, lipid mobilization, and the citric acid cycle—contain SNP associated with cows' ketosis resistance. Whereas GWAS have been conducted on both clinical and subclinical forms of ketosis, few studies have focused on the proxies of the cow's metabolism. Therefore, this study aimed to identify genomic regions associated with major hematic biomarkers of NEB in the Italian Holstein population and to provide a better understanding of the polygenic architecture of these traits in the first 35 d after calving. For this purpose, we used the blood concentration of BHB, NEFA, and urea predicted from milk mid-infrared (**MIR**) spectra.

MATERIALS AND METHODS

Blood Phenotypes

For this study, 6,190 Holstein clinically healthy cows raised in 374 herds across multiple regions covering most of the Italian territory were considered. In line with the official guidelines, on the day of the DHI milk testing, cows with clinical signs of disease or those who have recently received medical treatment were not sampled.

Between May 2020 and March 2023, spectral data from individual milk samples collected on the first test-day after calving (between 5 and 35 DIM) were provided for each cow by the Italian Breeders Association (AIA, Rome, Italy), which is in charge of the official milk recording routine in Italy. Milk samples were scanned using MilkoScan devices (Foss Electric A/S, Hillerød, Denmark), which on a regular basis undergo ring tests by the International Committee for Animal Recording. Milk spectra consisted of 1,060 wavelengths, which were used to predict BHB (log-transformed), NEFA (log-transformed), and blood urea using prediction models developed by Magro et al. (2025), whose R^2 were 0.64, 0.64, and 0.85, respectively. Additional fitting statistics and models' performance indicators are reported and widely described in Magro et al. (2024). The log-transformed values of BHB and NEFA were back-transformed using the following formula: $y = 10^{log\text{-}transformed}$, where y is the trait investigated. Descriptive statistics of both log-transformed and untransformed BHB, NEFA, and urea concentrations are reported in Table 1. Moreover, blood BHB was processed as a binary trait to identify SCK, with a value of "1" assigned if BHB was ≥1.20 mmol/L and "0" if it was <1.20 mmol/L.

Genotypes

Genomic data were provided by the Italian Holstein Association (ANAFBJ, Cremona, Italy), and, because

Table 2. Position and significance (*P*) of the SNP identified for log_{10}BHB, log_{10}NEFA, urea concentration, and subclinical ketosis (SCK)[1] predicted from mid-infrared milk spectra

Trait	BTA	SNP	Position (bp)	*P*
Log_{10}BHB	2	ARS-USMARC-Parent-DQ786757-rs29019900	110.396989	7.31E-05
	4	ARS-BFGL-NGS-12934	66.882641	6.36E-05
	6	BovineHD0600024859	89.048060	3.94E-05
	7	ARS-BFGL-NGS-37888	19.556429	5.14E-05
	18	BovineHD1800009244	29.811495	9.90E-05
	21	ARS-BFGL-NGS-1258	19.622207	2.45E-05
		Hapmap41010-BTA-52085	33.730093	6.08E-05
	22	BovineHD2200008741	30.212110	5.52E-05
	25	ARS-BFGL-NGS-100347	26.724480	3.87E-05
		ARS-BFGL-NGS-22050	26.052196	1.01E-06
		BovineHD2500008124	28.967999	4.73E-05
		Hapmap42993-BTA-59924	31.069863	8.98E-05
	28	ARS-BFGL-NGS-103144	13.354073	5.99E-07
		BovineHD2800003765	13.032275	4.87E-05
Log_{10}NEFA	1	Hapmap47450-BTA-96948	58.626471	3.73E-05
	4	Hapmap50445-BTA-70383	48.757663	5.18E-05
	13	ARS-BFGL-NGS-5210	67.003397	2.00E-05
	19	UA-IFASA-6043	30.422940	4.79E-06
Urea	16	ARS-BFGL-BAC-3576	26.114830	4.86E-05
	18	ARS-BFGL-NGS-3767	23.717174	5.88E-05
	25	BovineHD2500005262	18.616905	2.80E-05
SCK	1	BTB-01633151	155.792304	3.58E-06
	5	BovineHD0500011482	39.925033	8.03E-05
	11	BovineHD1100019193	67.895920	9.91E-05
	15	Hapmap41817-BTA-29310	15.336800	1.95E-05

[1]Healthy (5,849 cows): BHB <1.20 mmol/L. Affected (341 cows): BHB ≥1.20 mmol/L.

cows were genotyped with DNA chips of different brands and SNP density, genotypes were preliminarily imputed, resulting in 6,190 cows with 69,806 SNP from the BTA1 to BTA29.

The quality control was performed using the software PLINK 1.9 (Chang et al., 2015) by adopting standard quality checks aimed at removing SNP with call rate <90%, with minor allele frequency <1%, and deviating significantly (*P*-value < 1.00E-6) from the Hardy-Weinberg equilibrium. All the genotypes presented a call rate equal to or greater than 0.90. The linkage disequilibrium score (r^2) between 2 loci was calculated in PLINK 1.9. Whenever SNP pairs showed $r^2 > 0.80$ and were separated by ≤100,000 bp, only one of them was retained. After editing, 64,202 SNP for each cow were available for the GWAS.

Association Study

The linear mixed model approach implemented in GCTA software (Yang et al., 2011; Sahana et al., 2023) for the GWAS was

$$\mathbf{y} = \mu + \mathbf{X}\beta + \mathbf{H}\gamma + \mathbf{P}\delta + \mathbf{D}\rho + \mathbf{S}\varphi + \mathbf{u} + \boldsymbol{\varepsilon},$$

where **y** is the vector of phenotypes (log_{10}BHB, log_{10}NEFA, BHB, NEFA, urea, and binary BHB); μ is the intercept; **X** is a vector of marker genotypes; β is the effect size of the markers; **H**, **P**, **D**, and **S** are the incidence matrices for the fixed effect of herd-year (n = 1,261), parity (1 to 5), DIM (5 to 35), and sampling season (4 levels as: December to February, March to May, June to August, and September to November), with γ, δ, ρ, and φ being their corresponding regression coefficients; **u** is a vector of random individual effects; and **ε** is a vector of errors.

Log-likelihood ratio statistics were adopted to test the null hypothesis that a polymorphism did not affect the phenotype; that is, H0: $\beta = 0$ was tested against H1: $\beta \neq 0$ for each SNP. In addition, the genomic relationship matrix was included in the analysis to account for population structure and avoid the presence of systematic bias.

To identify the most significant SNP, 2 approaches were compared: the Bonferroni threshold and the false discovery rate (**FDR**). The first is usually considered too restrictive because of the assumption that SNP are all independent—thereby ignoring the linkage disequilibrium in multiple testing. The Bonferroni threshold leads to numerous false negative signals, especially in GWAS for polygenic complex traits where SNP effect size is generally small. The FDR with a cut-off at 0.20 ($P < 0.00013$) was used as a criterion to fulfill the *P*-value thresholds for significance discrimination (Efron, 2007). The FDR approach was considered in addition to the Bonferroni threshold, as it is less stringent and increases the likelihood of detecting potentially relevant

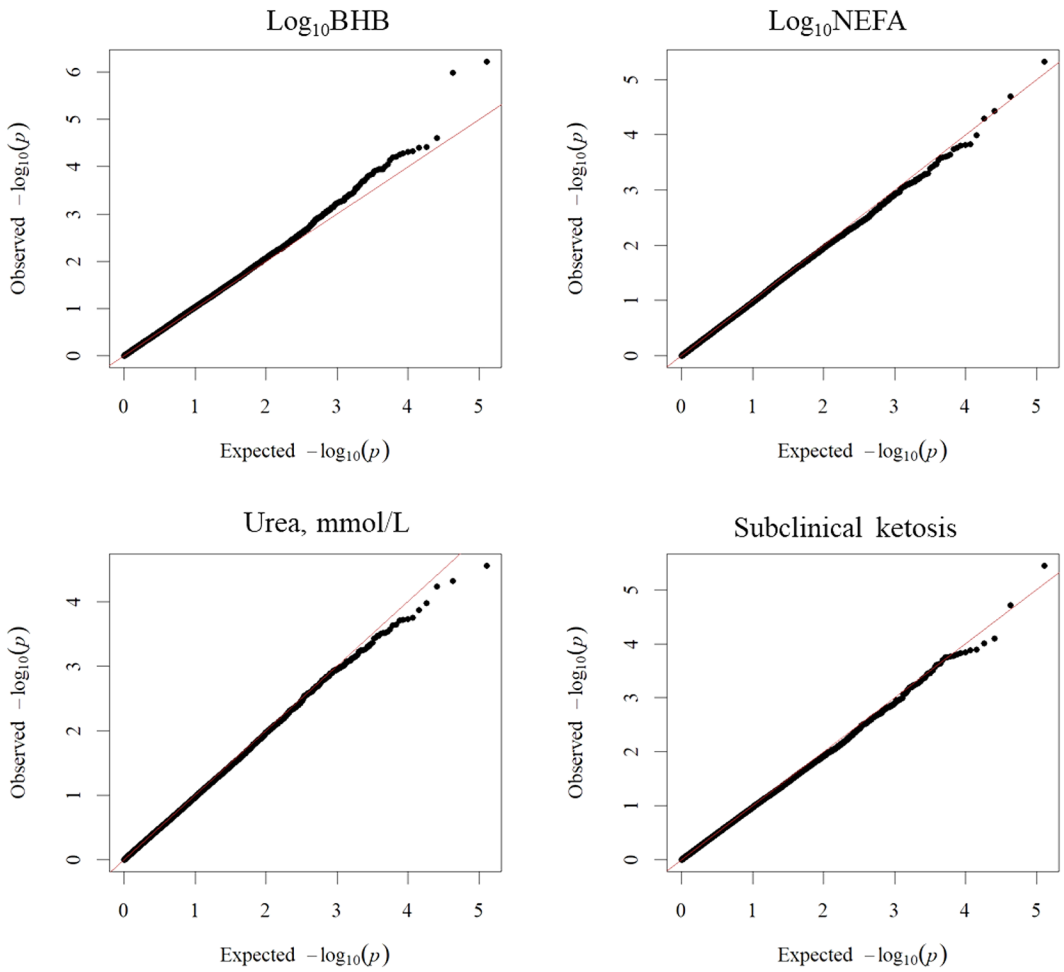

Figure 1. Quantile-quantile plot of the expected and the observed *P*-value distribution for $\log_{10}$BHB, $\log_{10}$NEFA, urea concentration, and subclinical ketosis. Concentration of $\log_{10}$BHB, $\log_{10}$NEFA, and urea concentration were predicted from milk mid-infrared spectra.

signals that might otherwise remain undetected under more conservative criteria.

Graphical representations of Manhattan and quantile-quantile plots were obtained in the R software using the "CMplot" (Yin, 2016) and "qqman" packages (S. D. Turner, University of Virginia School of Medicine, Charlottesville, VA, unpublished), respectively. Regions containing significant SNP were then used to identify genes located within or nearby these signals using the ENSEMBL Biomart Martview application (Ensembl Genes 97, http://www.ensembl.org/biomart/martview). Gene searches were performed using 2 distance thresholds from the significant SNP: a narrower window of ±0.1 Mb and a broader window of ±0.5 Mb to capture both closely and more distantly associated candidate genes. The reference *Bos taurus* genome assembly ARS-UCD 1.3 was used for the mapping.

Once genes were identified, a functional enrichment analysis was performed with DAVID (https://davidbioinformatics.nih.gov, Huang et al., 2008). Gene Ontology (**GO**) terms, which included cellular component (**CC**), molecular function (**MF**), biological process (**BP**), and the Kyoto Encyclopedia of Genes and Genomes (**KEGG**) pathways, were investigated, and those with $P < 0.05$ were considered significant. The enrichment results were subsequently visualized using a dot plot to illustrate the most relevant functional categories.

RESULTS

Blood BHB

In the present study, the blood punctual concentrations of biomarkers predicted via milk mid-infrared spectra were adopted. The $\log_{10}$BHB available for the 6,190 cows in early lactation (DIM ≤ 35) averaged −0.20, with a CV of 90.00%. Because BHB has skewed distribution,

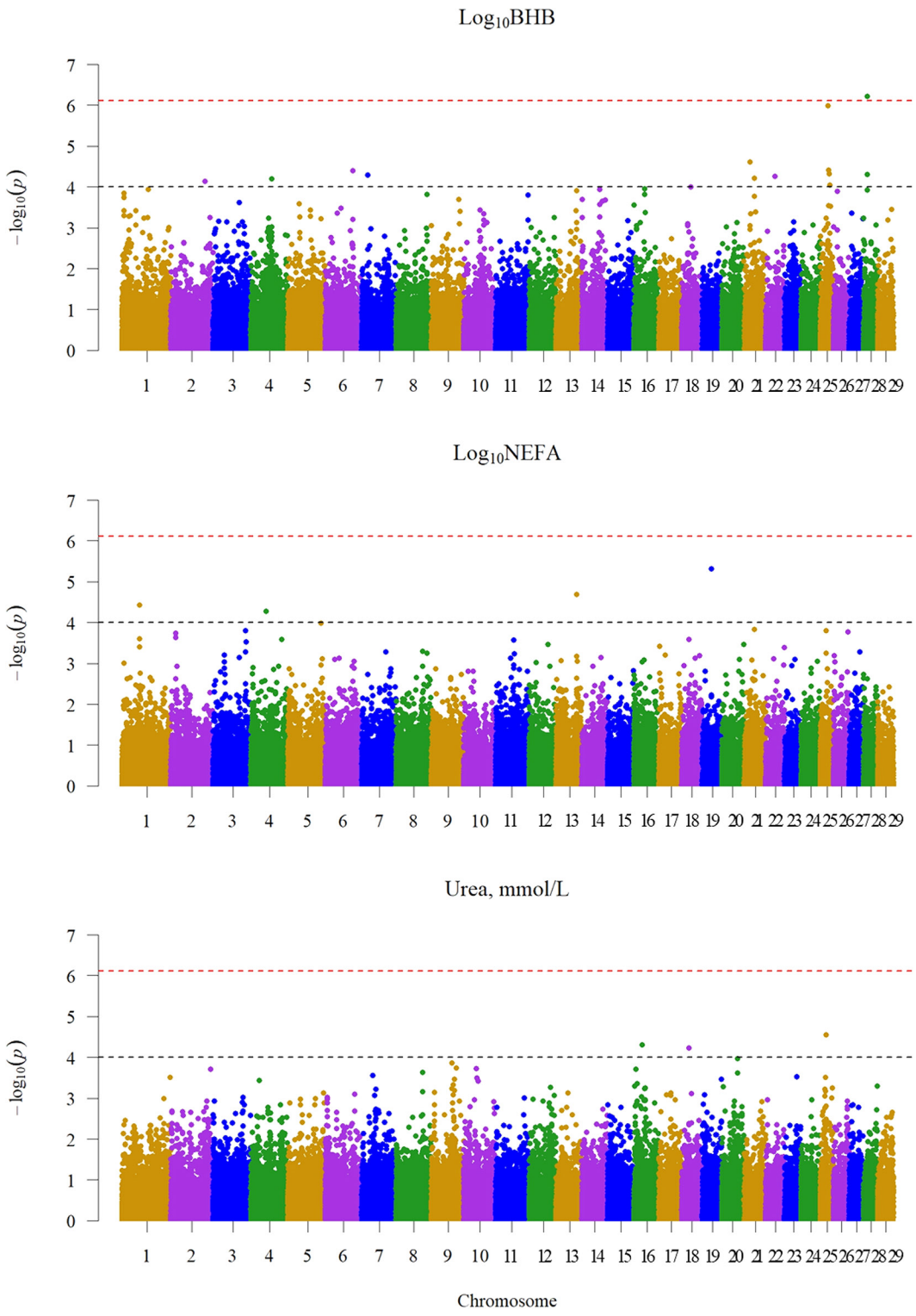

Figure 2. Manhattan plot for log_{10}BHB, log_{10}NEFA, and urea concentration predicted from mid-infrared milk spectra. The red and black dashed lines indicate Bonferroni and false discovery rate threshold, respectively.

Table 3. Gene harboring (Gene $_H$) the significant SNP for log_{10}BHB, log_{10}NEFA, and urea concentration along with nearby genes (left and right) for each signal

Trait	BTA	SNP	Gene $_H$	Nearby genes (±0.1 Mb from SNP)	Nearby genes (±0.5 Mb from SNP)
Log_{10}NEFA	1	Hapmap47450-BTA-96948	*ZDHHC23*	*GRAMD1C*, *CCDC191*	*QTRT2*, *DRD3*, *TIGIT*, *ZBTB20*, *CFAP44*, *SIDT1*, *USF3*, *NAA50*, *ATP6V1A*, *SPICE1*
Log_{10}BHB	2	ARS-USMARC-Parent-DQ786757-rs29019900	*PAX3*	*bta-mir-2284y-5*	*FARSB*, *SGPP2*
Log_{10}BHB	4	ARS-BFGL-NGS-12934	*CHN2*	—	*CPVL*, *CREB5*, *PRR15*, *SCRN1*, *TRIL*, *WIPF3*
Log_{10}NEFA	4	Hapmap50445-BTA-70383	*CBLL1*	*SLC26A4*, *SLC26A3*	*HBP1*, *COG5*, *GPR22*, *DUS4L*, *DLD*, *LAMB1*, *NRCAM*, *bta-mir-2418*
Log_{10}BHB	6	BovineHD0600024859	—	*CXCL2*, *CXCL3*, *MTHFD2L*, *GRO1*	*AFM*, *AREG*, *CXCL5*, *CXCL8*, *EPGN*, *EREG*, *RASSF6*
Log_{10}BHB	7	ARS-BFGL-NGS-37888	*SEMA6B*	*DPP9*, *MYDGF*, *TNFAIP8L1*, *LRG1*, *PLIN5*, *PLIN4*, *HDGFL2*	*ANKRD24*, *ARRDC5*, *CHAF1A*, *CREB3L3*, *DAPK3*, *EBI3*, *EEF2*, *FEM1A*, *FSD1*, *KDM4B*, *MAP2K2*, *MIR7–3*, *MPND*, *PIAS4*, *PLIN3*, *SH3GL1*, *SHD*, *SIRT6*, *SNORD37*, *STAP2*, *TICAM1* *TMIGD2*, *UBXN6*, *UHRF1*, *YJU2*, *ZBTB7A*
Log_{10}NEFA	13	ARS-BFGL-NGS-5210	*TGM2*	*TTI1*, *RPRD1B*, *KIAA1755*	*VSTM2L*, *BPI*, *LBP*, *RALGAPB*, *CTNNBL1*, *ADIG*, *SNORA71*
Urea	16	ARS-BFGL-BAC-3576	*MIA3*	*HHIPL2*, *TAF1A*, *AIDA*, *BROX*, *bta-mir-11975*	*FAM177B*, *DISP1*, *TLR5*, *U8*
Log_{10}BHB	18	BovineHD1800009244	—	*CDH8*	—
Urea	18	ARS-BFGL-NGS-3767	—	*MMP2*, *LPCAT2*	*IRX5*, *IRX6*, *SLC6A2*, *CES1*, *MT2A*, *GNAO1*, *BBS2*, *NUDT21*, *AMFR*
Log_{10}NEFA	19	UA-IFASA-6043	*DNAH9*	—	*SHISA6*, *ZNF18*, *MAP2K4*, *MIR744*
Log_{10}BHB	21	ARS-BFGL-NGS-1258	*ISG20*	*DET1*, *AEN*	*MRPL46*, *MRPS11*, *NTRK3*
Log_{10}BHB	21	Hapmap41010-BTA-52085	—	*PPCDC*, *SCAMP5*, *RPP25*, *COX5A*, *FAM219B*, *MPI*, *SCAMP2*	*ARID3B*, *bta-mir-631*, *C21H15orf39*, *CLK3*, *COMMD4*, *CPLX3*, *CSK*, *CYP1A1*, *CYP1A2*, *EDC3*, *IMP3*, *LMAN1L*, *MAN2C1*, *NEIL1*, *PTPN9*, *SIN3A*, *SNORA70*, *SNUPN*, *SNX33*, *UBL7*, *ULK3*
Log_{10}BHB	22	BovineHD2200008741	*FOXP1*	—	*bta-mir-1284*, *EIF4E3*, *GPR27*, *PROK2*
Log_{10}BHB	25	ARS-BFGL-NGS-100347	—	*ITGAL*, *ZNF688*, *PRR14*, *FBRS*, *ZNF689*	*ASPHD1*, *BCKDK*, *BCL7C*, *C16orf92*, *C25H16orf54*, *CD2BP2*, *CDIPT*, *CFAP119*, *CTF1*, *DCTPP1*, *DOC2A*, *FBXL19*, *HIRIP3*, *HSD3B7*, *INO80E*, *KAT8*, *KCTD13*, *KIF22*, *MAZ*, *MVP*, *MYL11*, *ORAI3*, *PAGR1*, *PHKG2*, *PRSS53*, *QPRT*, *RNF40*, *SEPTIN1*, *SETD1A*, *SEZ6L2*, *SNORA30*, *SPN*, *SRCAP*, *STX1B*, *STX4*, *TAOK2*, *TBC1D10B*, *TLCD3B*, *TMEM219*, *TMEM265*, *VKORC1*, *ZG16*, *ZNF48*, *ZNF629*, *ZNF646*, *ZNF668*, *ZNF771*
Log_{10}BHB	25	ARS-BFGL-NGS-22050	*CLN3*	*IL27*, *SGF29*, *NUPR1*, *SULT1A1*, *SLX1A*, *CORO1A*, *SH2B1*, *TUFM*, *ATXN2L*, *EIF3CL*	*ALDOA*, *ASPHD1*, *ATP2A1*, *ATXN2L*, *C16orf92*, *C25H16orf54*, *CD19*, *CD2BP2*, *CDIPT*, *DOC2A*, *GDPD3*, *GSG1L*, *HIRIP3*, *INO80E*, *KCTD13*, *KIF22*, *LAT*, *MAPK3*, *MAZ*, *MVP*, *NFATC2IP*, *NUPR1*, *PAGR1*, *PPP4C*, *QPRT*, *RABEP2*, *SBK1*, *SEZ6L2*, *SPN*, *SPNS1*, *TAOK2*, *TBC1D10B*, *TBX6*, *TLCD3B*, *TMEM219*, *XPO6*, *YPEL3*, *ZG16*
Log_{10}BHB	25	BovineHD2500008124	*CALN1*	—	*GALNT17*
Log_{10}BHB	25	Hapmap42993-BTA-59924	—	*AUTS2*, *U6*	—
Urea	25	BovineHD2500005262	*REXO5*	*ACSM3*, *ERI2*, *DCUN1D3*, *LYRM1*, *5S_rRNA*, *bta-mir-2384*	*ACSM5*, *ACSM2B*, *ACSM1*, *ACSM4*, *THUMPD1*, *DNAH3*, *LDAF1*, *ZP2*, *ANKS4B*, *CRYM*
Log_{10}BHB	28	BovineHD2800003765	*ZNF25*	*ZNF248*	*BMS1*, *CHRM3*, *CSGALNACT2*, *RET*, *ZNF33B*, *ZNF37A*
Log_{10}BHB	28	ARS-BFGL-NGS-5210	—	—	*BMS1*, *CSGALNACT2*, *FXYD4*, *HNRNPF*, *RASGEF1A*, *RET*, *ZNF248*, *ZNF25*, *ZNF37A*

the back-transformed BHB concentration has been investigated too, and its average in the whole dataset was 0.69 mmol/L (Table 1). The genomic h^2 estimated using the variance explained by all SNP for log_{10}BHB and back-transformed BHB were equal to 0.11 ± 0.02 and 0.10 ± 0.02, respectively (Table 1).

The significant polymorphisms detected for log_{10}BHB are listed in Table 2, and the quantile-quantile plot is

Table 4. Location, function, and process[1] of the genes harboring the significant SNP for log_{10}BHB, log_{10}NEFA, urea concentration, and subclinical ketosis[2]

Trait[2]	BTA	Gene	Window (Mb)	Function	Process
Log_{10}BHB	2	*PAX3*	110.37–110.47	DNA-binding transcription factor activity, RNA polymerase II-specific RNA polymerase II *cis*-regulatory region sequence-specific DNA binding	Anatomical development Regulation of transcription by RNA polymerase II
	4	*CHN2*	66.63–66.97	Gtpase activator activity	Positive regulation of gtpase activity Regulation of small gtpase mediated signal transduction Signal transduction
	7	*SEMA6B*	19.55–19.59	Chemorepellent activity Semaphorin receptor binding	Axon guidance Negative chemotaxis Negative regulation of axon extension Neural crest cell migration Positive regulation of cell migration Semaphorin-plexin signaling pathway
	21	*ISG20*	19.60–19.64	Exonuclease activity Nucleic acid binding	DNA and RNA catabolic process Defense response to virus Negative regulation of viral genome replication
	22	*FOXP1*	30.06–30.69	DNA-binding transcription repressor activity, RNA polymerase II-specific RNA polymerase II *cis*-regulatory region sequence-specific DNA binding	Regulation of transcription by RNA polymerase II
	25	*CLN3*	26.04–26.06		Lysosomal lumen acidification Lysosome organization
	25	*CALN1*	28.64–29.10	Calcium ion binding	
	28	*ZNF25*	13.02–13.05	DNA-binding transcription factor activity RNA polymerase II *cis*-regulatory region sequence-specific DNA binding	Regulation of transcription by RNA polymerase II
Log_{10}NEFA	1	*ZDHHC23*	58.62–58.63	Protein-cysteine S-palmitoyltranferase activity	Peptidyl-L-cysteine S-palmitoylation Protein targeting to membrane
	4	*CBLL1*	48.76–48.78	Ubiquitin protein ligase activity	Protein ubiquitination Regulation of cell adhesion
	13	*TGM2*	67.00–67.04	Protein-glutamine gamma-glutamyltransferase activity	Peptide cross-linking
	19	*DNAH9*	30.33–30.62	ATP binding ATP hydrolysis activity Dynein intermediate chain binding Dynein light intermediate chain binding Minus-end-directed microtubule motor activity	Microtubule-based movement
Urea	16	*MIA3*	26.10–26.16	Protein binding	Endoplasmic reticulum to golgi vesicle-mediated transport Protein secretion Vesicle cargo loading
	25	*REXO5*	18.56–18.63	RNA binding Exonuclease activity	
Subclinical ketosis	1	*CNTN1*	39.77–40.18	Cell adhesion mediator activity	Axon guidance Brain development Cell-cell adhesion
	11	*AAK1*	67.82–67.99	ATP binding Protein kinase activity	Protein phosphorylation
	15	*ENDOD1*	15.33–15.36	Hydrolase activity Metal ion binding Nucleic acid binding	

[1]Retreived from the National Center for Biotechnology Information website (https://www.ncbi.nlm.nih.gov/).

[2]Concentration of log_{10}BHB, log_{10}NEFA, and urea concentration were predicted from milk mid-infrared spectra, and subclinical ketosis was identified by considering the BHB threshold of 1.2 mmol/L.

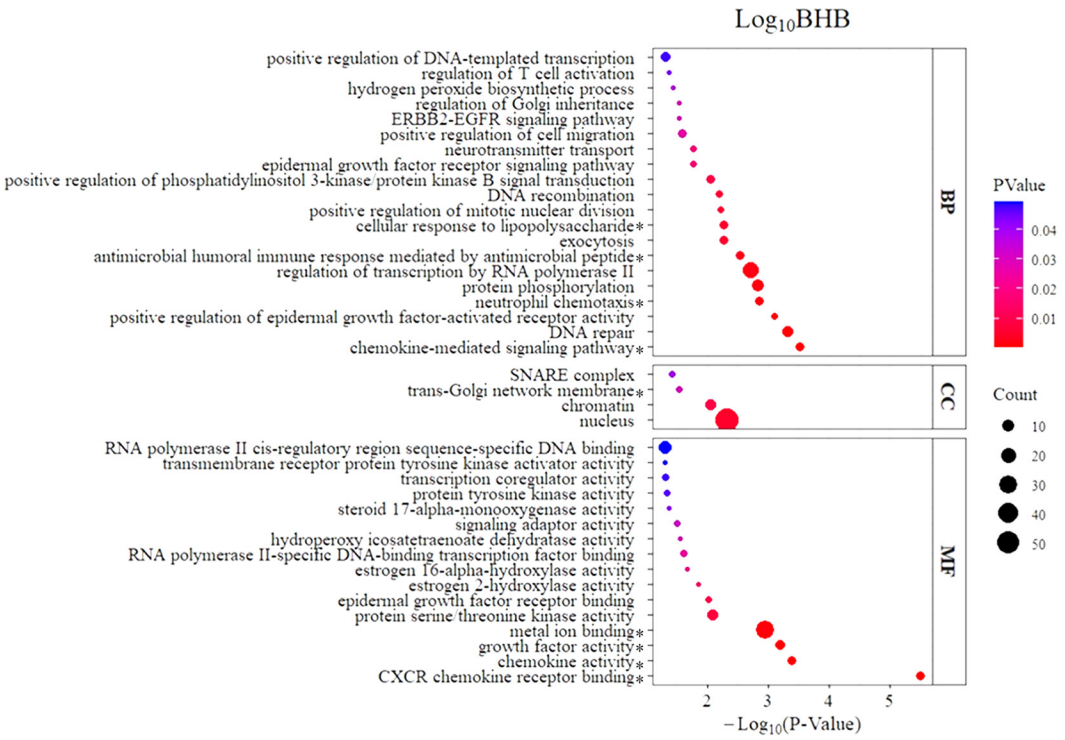

Figure 3. Gene Ontologies (GO) enriched for genes within 0.5 Mb flanking region of associated SNP for $\log_{10}$BHB predicted from mid-infrared milk spectra. The GO terms highlighted with an asterisk (*) correspond to genes detected within the narrower ±0.1 Mb region.

shown in Figure 1. Within the genome, signals of $\log_{10}$BHB were spread across several—often noncoding—DNA segments (Figure 2), with BTA21, 25, and 28 hosting multiple significant SNP.

In particular, BTA28 contained the most significant SNP, ARS-BFGL-NGS-103144, the only one that surpassed the Bonferroni threshold. However, this SNP fell within an intron, and even when looking at flanking regions (±0.1 Mb), no coding segments were observed. When considering a wider window (±0.5 Mb), several genes were found, such as *RET* and *BMS1*, as described in Table 3. In the same BTA, another significant SNP, BovineHD2800003765, fell within the *ZNF25* gene and, at the same time, near (±0.1 Mb) the *ZNF248* gene. Both genes are involved in the regulation of transcription by RNA polymerase II, with the first upregulating transcription and the second downregulating it (Table 4).

Other significant signals were detected in the region from 26.72 to 31.07 Mb of BTA25, with ARS-BFGL-NGS-22050 being the second most significant SNP in terms of *P*-value (Table 2), located within the *CLN3* gene, which is involved in lysosomal function (Table 4). In this region, another SNP inside the *CALN1* gene and nearby *GALNT17* gene was also significant (Tables 2 and 3).

An additional significant SNP was identified on BTA22 within *FOXP1*, a gene involved in the regulation of transcription by RNA polymerase II (Table 4). In BTA21, the *ISG20* gene was found to be significant (SNP ARS-BFGL-NGS-1258). This gene is involved in DNA and RNA catabolic processes, defense response to viruses, and negative regulation of viral genome replication (Table 4). In the same BTA, Hapmap41010-BTA-52085 fell near (±0.1 Mb) *AEN* and *DET1* genes (Table 3). The *AEN* gene enables exonuclease activity and nucleic acid binding, whereas *DET1* is involved in the positive regulation of proteasomal ubiquitin-dependent protein catabolic processes and protein ubiquitination. Other signals appeared in BTA2, 6, and 7, within *PAX3*, *CHN2*, and *SEMA6B*, respectively (Table 3).

The GWAS was also performed for the BHB concentration expressed in mmol/L, which was back-transformed from $\log_{10}$BHB (Supplemental Table S1 and Figure S1, see Notes) to isolate cows at risk using the conventional blood BHB threshold (1.20 mmol/L) and then evaluate if there is a genetic predisposition that makes cows highly susceptible to NEB and SCK. Overall, the genes identified for BHB were the same as $\log_{10}$BHB (Supplemental Table S2, see Notes), for example, *FOXP1* on BTA22, *CLN3* and *CALN1* on BTA25, and *ZNF25* on BTA28.

Genes ±0.1 Mb far from each significant SNP were used for GO enrichment and pathway analyses. The

Table 5. Kyoto Encyclopedia of Genes and Genomes (KEGG) pathways enriched for log_{10}BHB and urea concentration[1] positional candidate genes (genes within 0.5 Mb flanking region of associated SNP for log_{10}BHB or urea)[2]

Trait	KEGG	Pathway name	No. of genes	Gene names	*P*-value
Log_{10}BHB	bta04060	Cytokine-cytokine receptor interaction	8	*CTF1, CXCL8, EBI3, IL27, GRO1, CXCL3, CXCL2, CXCL5*	0.0467
	bta04061	Viral protein interaction with cytokine and cytokine receptor*	5	*CXCL8, GRO1, CXCL3, CXCL2, CXCL5*	0.0131
	bta04062	Chemokine signaling pathway	6	*CXCL8, GRO1, CXCL3, CXCL2, CXCL5, MAPK3*	0.0382
	bta04064	NF-kappa B signaling pathway*	7	*PIAS4, CXCL8, GRO1, CXCL3, TICAM1, CXCL2, LAT*	0.0008
	bta04621	NOD-like receptor signaling pathway	6	*CXCL8, GRO1, CXCL3, TICAM1, CXCL2, MAPK3*	0.0435
	bta04657	IL-17 signaling pathway*	6	*CXCL8, GRO1, CXCL3, CXCL2, CXCL5, MAPK3*	0.0023
	bta04668	TNF signaling pathway*	7	*CREB3L3, GRO1, CXCL3, CXCL2, CXCL5, MAPK3, CREB5*	0.0019
	bta05133	Pertussis	4	*CXCL8, TICAM1, CXCL5, MAPK3*	0.0401
	bta05134	Legionellosis*	4	*CXCL8, GRO1, CXCL3, CXCL2*	0.0187
	bta05135	Yersinia infection	6	*MAP2K2, CXCL8, WIPF3, TICAM1, LAT, MAPK3*	0.0178
	bta05161	Hepatitis B	6	*MAP2K2, CXCL8, CREB3L3, TICAM1, MAPK3, CREB5*	0.0327
	bta05167	Kaposi sarcoma-associated herpesvirus infection	7	*MAP2K2, CXCL8, GRO1, CXCL3, TICAM1, CXCL2, MAPK3*	0.0205
	bta05219	Bladder cancer	4	*MAP2K2, CXCL8, DAPK3, MAPK3*	0.0083
	bta05230	Central carbon metabolism in cancer	5	*RET, MAP2K2, NTRK3, SIRT6, MAPK3*	0.0045
	bta05323	Rheumatoid arthritis*	6	*CXCL8, ITGAL, GRO1, CXCL3, CXCL2, CXCL5*	0.0034
	bta05417	Lipid and atherosclerosis	7	*CXCL8, CYP1A1, GRO1, CXCL3, TICAM1, CXCL2, MAPK3*	0.0298
Urea	bta00650	Butanoate metabolism	5	*ACSM3, ACSM1, ACSM5, ACSM4, ACSM2B*	0.0004

[1]Concentration of log_{10}BHB and urea concentration were predicted from milk mid-infrared spectra.
[2]KEGG pathways highlighted with an asterisk (*) correspond to genes detected within the narrower ±0.1 Mb region.

genes were significantly enriched ($P < 0.05$) in 4 BP, 1 CC, and 4 MF (Figure 3), as well as in 6 KEGG pathways (Table 5). The chemokine-mediated signaling pathway (GO:0070098) was the most significantly enriched BP for log_{10}BHB (Figure 3). The trans-Golgi network membrane (GO:0032588) was the only enriched CC term detected for log_{10}BHB (Figure 3). Metal ion binding (GO:0046872) was the enriched MF with the highest number of genes (8) among the input genes. Meanwhile, CXCR chemokine receptor binding (GO: 0045236) was the most significantly enriched MF for log_{10}BHB (Figure 3). Finally, for this trait, rheumatoid arthritis was the most significant KEGG pathway (Table 5). When considering genes located ±0.5 Mb, significant enrichment ($P < 0.05$) was observed in 20 BP, 4 CC, and 16 MF (Figure 3), as well as in 14 KEGG pathways (Table 5).

Blood NEFA

The log_{10}NEFA averaged −0.53 with a CV of 83.02%. When values were back-transformed, the mean NEFA concentration was 0.49 mmol/L (Table 1). The genomic h^2 for both log_{10}NEFA and back-transformed NEFA was equal to 0.03 ± 0.01 (Table 1).

Significant SNP identified for log_{10}NEFA are shown in Table 2, and the quantile-quantile plot is shown in Figure 1. Although no SNP achieved the Bonferroni threshold, 4 signals were significant at the FDR threshold (Figure 2), with UA-IFASA-6043 in BTA19 falling within *DNAH9*, a gene associated with ATP binding and ATP hydrolysis activity (Table 4). The second significant SNP was located within the *TGM2* gene on BTA13. The *ZDHHC23* gene, involved in peptidyl-L-cysteine S-palmitoylation and protein targeting to the membrane (Table 4), was identified on BTA1, and *CBLL1* (BTA4), involved in protein ubiquitination and in the regulation of cell adhesion (Table 4), harbored a significant SNP.

The GWAS performed for NEFA concentration after back-transformation from log_{10}NEFA (Supplemental Table S1 and Figure S1) revealed findings consistent with those obtained using log_{10}NEFA values. In particular, the *ZDHHC23* gene on BTA1, *TGM2* on BTA13, and *DNAH9* on BTA19 were identified. Additionally, significant SNP were found within *DIS3L* on BTA10 and within *SRC* on BTA13 (Supplemental Table S2).

Independently of the window size applied (±0.1 Mb or ±0.5 Mb), genes were significantly enriched ($P < 0.05$) in 1 BP and several MF (Figure 4). Specifically, when considering the ±0.1 Mb window, 5 MF and 1 BP were identified, whereas using the broader ±0.5 Mb window resulted in the detection of one additional MF. No KEGG pathways were detected.

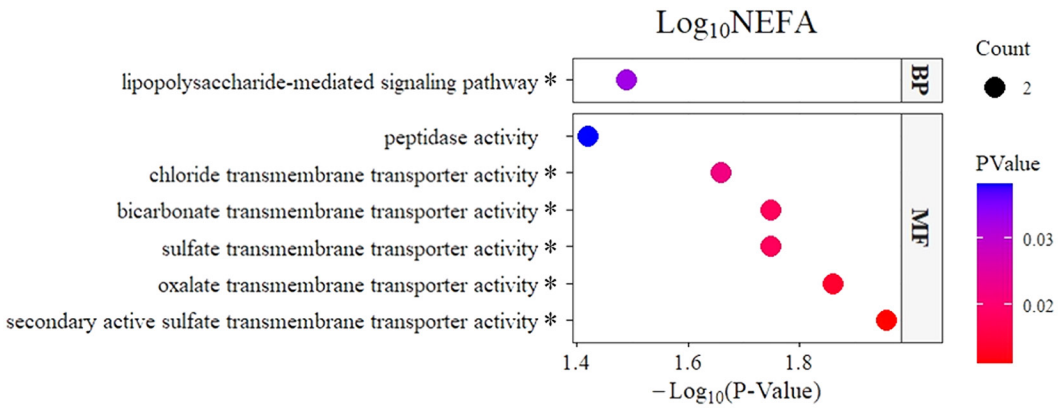

Figure 4. Gene Ontologies (GO) enriched for genes within 0.5 Mb flanking region of associated SNP for log_{10}NEFA predicted from mid-infrared milk spectra. The GO terms highlighted with an asterisk (*) correspond to genes detected within the narrower ±0.1 Mb region.

Blood Urea

The average blood urea concentration in this study was 2.63 mmol/L, with a CV of 59.70%, and the genomic h^2 was 0.06 ± 0.02 (Table 1). The details of all significant SNP are listed in Table 2, and the quantile-quantile plot is shown in Figure 1. For this trait, only 3 signals on BTA16, BTA18, and BTA25 reached the FDR threshold (Figure 2). BovineHD2500005262 on BTA25 was located in *REXO5*, a gene involved in RNA binding and exonuclease activity (Table 4). Additionally, a significant SNP was identified on BTA16 within *MIA3*, a gene associated with protein binding (Table 4). On BTA18, the SNP ARS-BFGL-NGS-3767 was located near (±0.1 Mb) *MMP2* and *LPCAT2* genes (Table 3).

Considering a window of ±0.1 Mb, the GO enrichment and pathway analyses for urea concentration did not reveal any significant enrichment, likely due to the small number of genes identified. However, when considering genes within ±0.5 Mb, significant enrichment ($P < 0.05$) was observed in 3 BP, 3 CC, and 5 MF (Figure 5), and only one KEGG pathway was identified (Table 5).

Subclinical Ketosis

To detect variants associated with SCK and carry out the GWAS on a dichotomous variable, cows were classified as healthy if BHB concentration was <1.20 mmol/L (5,849 cows) and suspected of SCK if ≥1.20 mmol/L (341 cows), 204 of which (60%) were sampled within 14 DIM, indicating that BHB frequently exceeded the conventional threshold in the first 2 wk of lactation.

As observed for the other traits, the genomic h^2 for this binary trait was low, too (0.03; Table 1). The significant variants are listed in Table 2, and the quantile-quantile plot is shown in Figure 1. Whereas no SNP were significant with the Bonferroni threshold, 4 signals in different BTA surpassed the FDR threshold (Figure 6). In particular, BTB-01633151 in a noncoding segment of BTA1 was the most significant SNP for SCK. Whereas no coding regions were detected within the initial ±0.1 Mb window, extending the range to ±0.5 Mb allowed for the identification of *SATB1* (Figure 6). A significant SNP on BTA5 was within *CNTN1*, a gene with cell adhesion mediator activity (Table 4), and another one fell within *AAK1* in BTA11, a gene involved in protein phosphorylation (Table 4). The signal on BTA14 was within the *ENDOD1*, which regulates hydrolase activity (Table 4), metal ion binding, and nucleic acid binding. In the flanking region of this SNP, there was the *SESN3* gene, which regulates L-leucine binding and oxidoreductase activity and acts on peroxides as acceptors (Table 4).

The GO enrichment and pathway analysis for this binary trait, considering both the ±0.1 Mb and ±0.5 Mb windows, revealed no significant enrichment, likely due to the limited number of genes identified.

DISCUSSION

Prediction of complex traits through milk MIR spectra is useful in populations lacking sufficient phenotypes, allowing for monitoring on a large scale. The blood traits investigated in the present study were predicted using milk MIR spectra using the prediction equations published by Magro et al. (2025). Although the response to genetic selection using proxies is generally lower than that achievable with directly observed phenotypes (Chesnais et al., 2016), it still allows selection within a given population to progress in the desired direction. In the present study, the predicted blood traits were used at the genomic level to identify genomic signals potentially associated with metabolites related to energy balance (BHB, NEFA, urea) and SCK.

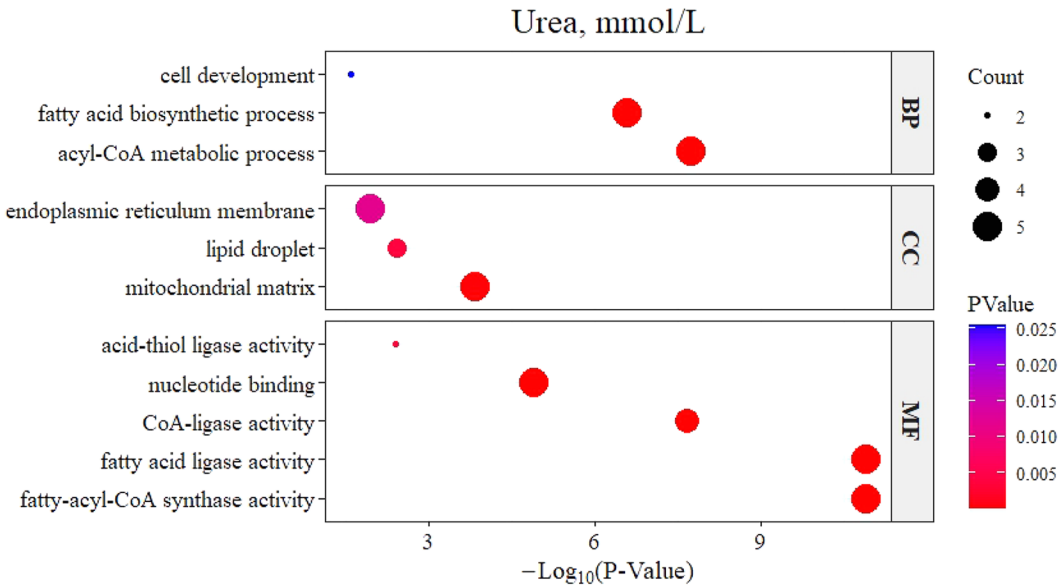

Figure 5. Gene Ontologies (GO) enriched for genes within 0.5 Mb flanking region of associated SNP for urea concentration predicted from mid-infrared milk spectra.

In this study, the genomic h^2 for predicted hematic traits were generally low (<0.11; Table 1), but these are consistent with previously reported estimates for other health traits in dairy cattle. Most of the studies to date have reported the pedigree-based h^2 estimates, which, however, do not consider the Mendelian sampling. For example, the pedigree-based h^2 was 0.078 for clinical ketosis in Norwegian Red cows (Belay et al., 2017) and 0.13 for blood BHB, 0.03 for blood NEFA, and 0.04 for blood urea in Italian Holsteins (Magro et al., 2025).

The GWAS demonstrated that there were significant signals for our infrared-predicted hematic traits along the *Bos taurus* genome, confirming the polygenic nature and complex architecture of the blood concentration of these biomarkers in clinically healthy animals during the early lactation, a period commonly associated with NEB. This finding aligns with the emerging view that ketone bodies act as signaling molecules involved in the regulation of metabolic health, immune function, and physiological resilience in dairy cows (Rico and Barrientos-Blanco, 2024).

Log-transformed traits such as BHB were analyzed along with the back-transformed values (expressed in mmol/L, nonnormally distributed) to compare significant SNP, regions, and genes. The GWAS was carried out for SCK, a binary qualitative trait that indicates the presence of hyperketonemia (BHB ≥1.20 mmol/L; Benedet et al., 2019). Table 3 summarizes the detected genes with signals located within or near gene regions, using 2 window sizes (±0.1 Mb and ±0.5 Mb). The larger window (±0.5 Mb) identified a substantially greater number of genes.

Two significance thresholds were used, adopting less stringent criteria (i.e., Bonferroni and FDR), in line with previous studies on similar low h^2 traits (Nayeri et al., 2019; Klein et al., 2020). This approach was chosen to increase the sensitivity of detection and to capture potentially informative associations that might otherwise be overlooked under more conservative thresholds. These signals, although requiring further validation, can provide valuable insights for subsequent biological interpretation and hypothesis generation.

Blood BHB

The scattered fragmented signals observed along the genome and the biological functions of the candidate genes confirmed the complex nature of $\log_{10}$BHB, as also supported by the Q-Q plot, where only a few SNP deviate from the null expectation (Figures 1 and 2). Some regions and genes identified for this trait in this study have already been reported in previous GWAS for SCK. For example, *CLN3* on BTA25 was already reported by Nayeri et al. (2019) as a candidate gene for SCK in multiparous Canadian Holsteins. Although scarcely studied so far, this gene is reported to indirectly regulate lipids and proteins degradation by directly acting on the lysosomal functions and enzymes production (Schmidtke et al., 2019).

Buggiotti et al. (2021) observed that *FOXP1* (BTA22) acts as a transcriptional repressor and plays a key role in the regulation of systemic glucose homeostasis (Zou et al., 2015), and that its expression increased with parity of the

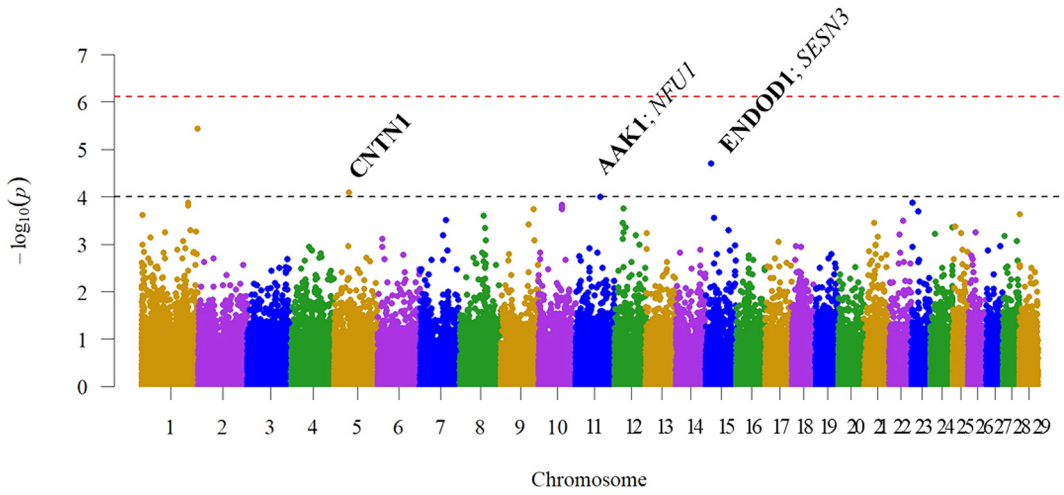

Figure 6. Manhattan plot for subclinical ketosis (healthy: BHB <1.20 mmol/L.; affected: BHB ≥1.20 mmol/L) and gene and gene harboring the significant SNP (in bold writing) and the nearby genes (±0.1 Mb from SNP) on the left and right (in italics). The red and black dashed lines indicate Bonferroni and false discovery rate threshold, respectively. Nearby genes (±0.5 Mb from SNP) included *SATB1* on BTA1, *PDZRN4* on BTA5, *GFPT1*, *ANXA4*, *GMCL1*, *MXD1*, *ANTXR1*, and *ASPRV1* on BTA11, as well as *CWC15* and *AMOTL1* on BTA15.

cow, based on the transcriptome derived from RNA-seq data of leukocytes. This is particularly relevant because multiparous cows are at higher risk of metabolic disorders than primiparous cows; for instance, the higher prevalence of hyperketonemia in older cows is largely attributed to greater milk production and the metabolic stress carried over from previous lactations (Benedet et al., 2019).

Wathes et al. (2009) reported that *ISG20* located on BTA21, along with other genes associated with IFN (e.g., *MX1*, *MX2*, *IFIH1*, *GBP1*, and *Loc512486*) were upregulated in cows experiencing severe NEB and cows undergoing an active uterine inflammatory response 2 wk postpartum, based on RNA isolated from uterine tissue. During the transition period, dairy cows with hyperketonemia experience immune dysfunction, which is often considered the main cause of their high vulnerability to infectious diseases such as metritis and mastitis (Aleri et al., 2016; Horst et al., 2021). Wathes et al. (2021) reported that *SEMA6B* on BTA7, a gene with roles in immune signaling, was highly expressed in Holstein cows in early lactation with high IGF-1 levels in blood (>100 ng/mL), based on leukocyte transcriptomes analyzed using RNA sequencing.

A significant SNP for $\log_{10}$BHB on BTA6 was located near several genes (within ±0.1 Mb), namely *GRO1*, *CXCL2*, and *CXCL3* (Table 3). These have different MF, are involved in various BP, and are associated with distinct KEGG pathways, all related to the immune system and response (Figure 3; Table 5), such as the chemokine-mediated signaling pathway (GO:0070098), cellular response to LPS (GO:0071222), antimicrobial humoral immune response mediated by antimicrobial peptide (GO:0061844), and neutrophil chemotaxis (GO:0030593). Additionally, these genes exhibit chemokine activity (GO:0008009), growth factor activity (GO:0008083), and CXCR chemokine receptor binding (GO:0045236). These MF and BP were the most significant in the GO analysis of $\log_{10}$BHB. These findings suggest that immune-related genes may play an important role in the cow's NEB and in the occurrence of SCK. Inflammatory signaling may be both a consequence of metabolic stress and a contributor to further metabolic imbalances, creating a feedback loop that worsens the condition. This aligns with previous studies highlighting the overlap between metabolic and immune pathways in transition dairy cows (Bradford et al., 2015; Trevisi and Minuti, 2018). Nonetheless, current evidence does not support a direct causal relationship between hyperketonemia and the development of inflammation, and further research is needed to clarify the nature and direction of this association (Horst et al., 2021; Rico and Barrientos-Blanco, 2024).

Genes such as *GRO1*, *CXCL2*, and *CXCL3* in BTA6 were enriched in different pathological pathways (Table 5), including infectious legionellosis and rheumatoid arthritis, due to their involvement in immune and inflammatory responses.

"Regulation of transcription by RNA polymerase II" (GO:0006357), the BP most enriched in genes associated with $\log_{10}$BHB, encompassed several genes located within ±0.5 Mb on BTA2, 4, 7, 21, 22, 25, and 28. Under NEB conditions, these genes may modulate the expression of other genes involved in the metabolism of lipids and carbohydrates and energy production in response to metabolic stress during early lactation (Zhang et al., 2016).

Several genes, including those directly harboring one or more significant SNP (e.g., *CHN2* on BTA4, *FOXP1*

on BTA22, and *ZNF25* on BTA28), shared the MF of metal ion binding (GO:0046872; Figure 3). This function is particularly relevant in the context of NEB, as several enzymes involved in lipid metabolism and energy homeostasis can be influenced or regulated by metal ions (e.g., zinc, iron, or magnesium) which act as cofactors or structural stabilizers in numerous metabolic pathways. Expression of these genes may therefore influence the activity of metal ion, regulated metabolic enzymes, thereby affecting the cow's ability to mobilize lipids during NEB (Kostenkova et al., 2022).

CALN1 on BTA25 and *SCAMP5* and *SCAMP2* on BTA21 are associated with the CC of the trans-Golgi network membrane (GO:0032588; Figure 3), which plays a fundamental role in the selection, sorting, and transport of proteins and vesicles to their final destinations (von Blume and Hausser, 2019). Alterations in these cellular processes may disrupt lipid and energy metabolism, potentially impairing the liver's ability to process the large influx of fatty acids mobilized from adipose tissue during NEB, compromising lipoprotein secretion and affecting mitochondrial function and β-oxidation (Surma et al., 2012). Moreover, Matenchi et al. (2025) reported that *CALN1* plays a role in feed efficiency and lipid metabolism, and therefore it should be considered a candidate gene for the improvement of growth in cattle.

Overall, various signals did not surpass the significance threshold, some of which were genes historically important for dairy cattle, e.g., the *ARS-BFGL-NGS-4939* within the *DGAT1* on BTA14. The *DGAT1* gene, in fact, is known for its role in fat metabolism and inflammatory response in dairy cattle (Xu et al., 2022) and has been found in previous studies on SCK detected through milk BHB (Nayeri et al., 2019) or ketosis (Freebern et al., 2020).

Blood NEFA

For $\log_{10}$NEFA, the number of significant SNP was low, covering only BTA1, 4, 13, and 19 (Table 2; Figure 2), consistent with the quantile-quantile plot showing no evidence of strong signals (Figure 1). Although NEFA are commonly used as indicators of SCK (Ospina et al., 2010), the limited genetic signal observed here likely reflects phenotypic imprecision rather than a true lack of genetic variability. The traits under study were mid-infrared predicted from milk by using prediction equations whose accuracy in external validation was far from unity (e.g., for the concentration of NEFA, the R^2 was 0.54). Because NEFA concentration varies markedly with feeding and metabolic status (Seely et al., 2021), a single daily blood sample may not accurately capture the individual's peak value, thereby affecting phenotypic and genetic variance.

The *TGM2* gene on BTA13, which was significant for $\log_{10}$NEFA, was also reported by McCarthy et al. (2010), who observed that its expression in the aryl hydrocarbon receptor signaling pathway is part of the network involving lipid metabolism, molecular transport, and small molecule biochemistry, and is downregulated in cases of severe NEB. *TGM2* (BTA13) and *CFAP44* on BTA1 (gene located within ±0.5 Mb) were involved in peptidase activity (GO:00082333; Figure 4). This function may be relevant in skeletal muscle tissues during metabolic stress, where inflammatory signaling and proteolysis are activated, and peptidases contribute to the degradation of endogenous proteins to supply alternative energy substrates (Sadri et al., 2023).

The significant *SLC26A4* and *SLC26A3* genes on BTA4 (Table 3) are involved in the transmembrane transport of sulfate (GO:0015116), secondary active sulfate (GO:0008271), oxalate (GO:0019531), chloride (GO:0015108), and bicarbonate (GO:0015106; Figure 4). These solute carrier genes are involved in maintaining ionic and acid-base homeostasis, which is critical during periods of metabolic stress, such as early lactation.

Blood Urea

The literature reports that blood urea concentrations are more affected by management factors (especially feeding) than the genetic one (Lavery and Ferris, 2021). In this study, only 3 signals in different BTA were significant (Table 2; Figure 2). These results are also supported by the quantile-quantile plot, where no evidence of association is observed (Figure 1).

When considering genes within a narrow window of ±0.1 Mb, only a few genes were detected, and no GO terms were obtained. Conversely, when using the broader window of ±0.5 Mb, the significant SNP on BTA25 was near the *ACSM* family of genes, that is, *ACSM3*, *ACSM1*, *ACSM5*, *ACSM4*, and *ACSM2B* (Table 3). These coding regions have different MF and are involved in various BP. In particular, they exhibit fatty acyl-CoA synthase activity (GO:0004321), fatty acid ligase activity (GO:0015645), CoA ligase activity (GO:0016405), acid-thiol ligase activity (GO:0016878), and nucleotide binding (GO:0000166). Moreover, these genes participate in fatty acid biosynthetic process (GO:0006633) and acyl-CoA metabolic process (GO:0006637). Their association with hematic urea concentration suggests a link between lipid metabolism and nitrogen balance during the transition period in dairy cows, when energy demands increase, but feed intake tends to decrease (Grummer et al., 2004; González et al., 2011).

The findings can only be compared with the results of van den Berg et al. (2022), who carried out a GWAS for blood urea predicted using mid-infrared spectroscopy in

2,000 cows. The authors reported the presence of QTL on BTA2, 3, 9, 11, 12, and 14. In this study, various SNP on BTA9 were observed, but they did not surpass the significance threshold.

Subclinical Ketosis

It is worth highlighting that, although all cows were clinically healthy, some individuals exhibited BHB concentrations above the critical threshold (≥1.20 mmol/L). Therefore, these animals were classified as "at risk," and a binary variable was created by assigning a value of "1" to cows with BHB levels above the threshold and "0" to those below it. For this trait, only a few signals were detected (Figures 1 and 2), which did not share common genes/regions with $\log_{10}$BHB. These 2 distinct traits convey complementary biological information and are expected to be governed by different genetic mechanisms, given that the $\log_{10}$BHB data in this study were obtained from healthy cows—whether fully or partially within physiological ranges—thus reflecting the inherent, continuous variability present in the population. Therefore, the variability of this continuous trait considers the normal variation in cows. In contrast, the binary trait SCK distinguishes 2 groups of cows: low versus high blood BHB (< and ≥1.20 mmol/L, respectively).

The *CNTN1* on BTA5 was also reported by Ning et al. (2023) in a differential expression analysis of subcutaneous white adipose tissue from 10 Holstein cows classified as "at risk" and 10 healthy cows based on blood BHB levels. This gene was identified as being involved in the positive regulation of synaptic development and cell adhesion.

The *AAK1* gene on BTA11 was highlighted by Lee et al. (2024) in a GWAS conducted on 112 Holstein cows, analyzing the incidence of SCK (BHB ≥ 1.20 mmol/L) between 5 and 18 DIM.

Kim et al. (2022) observed that the expression of genes related to glucose metabolism, including the gene *SESN3* in this study significant for SCK (Figure 6), decreased in the late fattening phases in Japanese Black steers. This suggests that the coding region is involved in lipid metabolism in cattle.

CONCLUSIONS

This study identified genomic regions associated with metabolic biomarkers in early-lactation Holstein cows. Genome-wide signals and candidate gene functions support the complex polygenic architecture of blood metabolites, whereas associations for SCK were concentrated in fewer regions related to metabolism and immune response. The lack of overlapping regions among traits highlights their distinct physiological background. Compared with continuous metabolite measures, the binary phenotype enabled clearer genetic differentiation (i.e., cows above or below the diagnostic threshold) linked to susceptibility to this metabolic disorder. Because health traits are generally lowly heritable, the cows involved were apparently healthy and our phenotypes were predicted from mid-infrared milk spectra rather than direct blood measurements, further validation is advisable. Overall, these results provide new insights into the genetic mechanisms underlying NEB and SCK and suggest promising targets for future functional studies and potential genetic improvement strategies.

NOTES

This study received support from the project "Ketogen" of the Breeders Association of Veneto Region (ARAV, Vicenza, Italy) funded in 2022. Authors thank farmers for joining the study, ARAV for providing milk sample data, and the Italian Holstein Association (ANAFIBJ, Cremona, Italy) for the technical support. The software "Paperpal" by Editage was used for proofreading the final version of the manuscript. Supplemental material for this article is available at https://doi.org/10.6084/m9.figshare.30581483. Because no human or animal subjects were used, this analysis did not require approval by an Institutional Animal Care and Use Committee or Institutional Review Board. The authors have not stated any conflict of interest.

Nonstandard abbreviations used: BP = biological process; CC = cellular component; FDR = false discovery rate; GO = Gene Ontology; KEGG = Kyoto Encyclopedia of Genes and Genomes; MF = molecular function; MIR = mid-infrared spectra; NEB = negative energy balance; NEFA = nonesterified fatty acids; SCK = subclinical ketosis.

REFERENCES

Aleri, J. W., B. C. Hine, M. F. Pyman, P. D. Mansell, W. J. Wales, B. Mallard, and A. D. Fisher. 2016. Periparturient immunosuppression and strategies to improve dairy cow health during the periparturient period. Res. Vet. Sci. 108:8–17. https://doi.org/10.1016/j.rvsc.2016.07.007.

Belay, T. K., M. Svendsen, Z. M. Kowalski, and T. Ådnøy. 2017. Genetic parameters of blood β-hydroxybutyrate predicted from milk infrared spectra and clinical ketosis, and their associations with milk production traits in Norwegian Red cows. J. Dairy Sci. 100:6298–6311. https://doi.org/10.3168/jds.2016-12458.

Benedet, A., A. Costa, M. De Marchi, and M. Penasa. 2020. Heritability estimates of predicted blood β-hydroxybutyrate and nonesterified fatty acids and relationships with milk traits in early-lactation Holstein cows. J. Dairy Sci. 103:6354–6363. https://doi.org/10.3168/jds.2019-17916.

Benedet, A., C. L. Manuelian, A. Zidi, M. Penasa, and M. De Marchi. 2019. Invited review: β-hydroxybutyrate concentration in blood and

milk and its associations with cow performance. Animal 13:1676–1689. https://doi.org/10.1017/S175173111900034X.

Bradford, B. J., K. Yuan, J. K. Farney, L. K. Mamedova, and A. J. Carpenter. 2015. Invited review: Inflammation during the transition to lactation: New adventures with an old flame. J. Dairy Sci. 98:6631–6650. https://doi.org/10.3168/jds.2015-9683.

Buggiotti, L., Z. Cheng, M. Salavati, C. D. Wathes, A. Fahey, A. Crisà, A. Fouladi, A. Wylie, A. Vanlierde, A. Fogh, A. Santoro, A. Cromie, A.-S. Van Laere, A. Pearn, A. Evertson, A. Laine, B. S. Bernardo, B. Moioli, B. Vanranst, C. Bastin, C. Gaillard, C. Tan, C. Elsik, C. Marchitelli, C. Wathes, C. Grelet, C. Byrne, C. Ferris, D. Matthews, D. Triant, D. Werling, E. Matthews, E. Meyer, E. Froidmont, F. Signorelli, F. Carter, F. Napolitano, F. Kearney, F. Becker, F. Colinet, F. Dehareng, G. Conant, G. Opsomer, G. Pollott, G. Wang, G. Hua, H. Bogaert, H. Takeda, H. Hammami, H. Chen, J. Vandepitte, J. Rothmann, J. Ettema, J. De Koster, J. McClure, J. Taylor, J. Hoglund, J. Zhao, K. Ingvartsen, K. Hermans, L. Vandevelde, L. Foldager, L. Yang, L. Kosten, L. Buttazzoni, M. R. Pamplona, M. Crowe, M. Sciarretta, M. Schulze, M. T. Sorensen, M. Bell, M. McClure, M. Lucy, M. Salavati, M. Bonneau, M. Georges, M. Vaneetvelde, M. Hostens, M. Krogh, N. McLoughlin, N. Gengler, P. Rudd, R. Mota, R. O'Flaherty, S. N. Darbagshahi, S. Moerman, S. P. Vera, S. Zhang, S. Hallinan, S. Ostergaard, S. Dahl, T. Andersen, T. Rousing, T. Larsen, V. H. Silva de Oliveira, X. Chen, and Z. Cheng. 2021. Comparison of the transcriptome in circulating leukocytes in early lactation between primiparous and multiparous cows provides evidence for age-related changes. BMC Genomics 22:693. https://doi.org/10.1186/s12864-021-07977-5.

Carbon, S., A. Ireland, C. J. Mungall, S. Shu, B. Marshall, S. Lewis, and AmiGo Hub. 2009. AmiGO: Online access to ontology and annotation data. Bioinformatics 25:288–289. https://doi.org/10.1093/bioinformatics/btn615.

Chang, C. C., C. C. Chow, L. C. Tellier, S. Vattikuti, S. M. Purcell, and J. J. Lee. 2015. Second-generation PLINK: Rising to the challenge of larger and richer datasets. Gigascience 4:s13742-015-0047-8. https://doi.org/10.1186/s13742-015-0047-8.

Chesnais, J. P., T. A. Cooper, G. R. Wiggans, M. Sargolzaei, J. E. Pryce, and F. Miglior. 2016. Using genomics to enhance selection of novel traits in North American dairy cattle. J. Dairy Sci. 99:2413–2427. https://doi.org/10.3168/jds.2015-9970.

Costa, A., S. Magro, S. Sterup Moore, G. Visentin, M. Penasa, and M. De Marchi. 2024. Milk as diagnostic medium for detection of health disorders in dairy animals. Pages 557–570 in Production Diseases in Farm Animals: Pathophysiology, Prophylaxis and Health Management. Cham: Springer International Publishing.

Efron, B. 2007. Size, power and false discovery rates. Ann. Stat. 35:1351–1377. https://doi.org/10.1214/009053606000001460.

Freebern, E., D. J. Santos, L. Fang, J. Jiang, K. L. Parker Gaddis, G. E. Liu, P. M. VanRaden, C. Maltecca, J. B. Cole, and L. Ma. 2020. GWAS and fine-mapping of livability and six disease traits in Holstein cattle. BMC Genomics 21:41. https://doi.org/10.1186/s12864-020-6461-z.

González, F. D., R. Muiño, V. Pereira, R. Campos, and J. L. Benedito. 2011. Relationship among blood indicators of lipomobilization and hepatic function during early lactation in high-yielding dairy cows. J. Vet. Sci. 12:251–255. https://doi.org/10.4142/jvs.2011.12.3.251.

Grummer, R. R., D. G. Mashek, and A. Hayirli. 2004. Dry matter intake and energy balance in the transition period. Vet. Clin. North Am. Food Anim. Pract. 20:447–470. https://doi.org/10.1016/j.cvfa.2004.06.013.

Horst, E. A., S. K. Kvidera, and L. H. Baumgard. 2021. Invited review: The influence of immune activation on transition cow health and performance—A critical evaluation of traditional dogmas. J. Dairy Sci. 104:8380–8410. https://doi.org/10.3168/jds.2021-20330.

Huang, D. W., B. T. Sherman, and R. A. Lempicki. 2008. Systematic and integrative analysis of large gene lists using DAVID bioinformatics resources. Nat. Protoc. 4:44–57. https://doi.org/10.1038/nprot.2008.211.

Kim, M., T. Masaki, K. Ikuta, E. Iwamoto, Y. Uemoto, F. Terada, and S. Roh. 2022. Changes in the liver transcriptome and physiological parameters of Japanese Black steers during the fattening period. Sci. Rep. 12:4029. https://doi.org/10.1038/s41598-022-08057-8.

Klein, S. L., C. Scheper, K. May, and S. König. 2020. Genetic and non-genetic profiling of milk β-hydroxybutyrate and acetone and their associations with ketosis in Holstein cows. J. Dairy Sci. 103:10332–10346. https://doi.org/10.3168/jds.2020-18339.

Kostenkova, K., G. Scalese, D. Gambino, and D. C. Crans. 2022. Highlighting the roles of transition metals and speciation in chemical biology. Curr. Opin. Chem. Biol. 69:102155. https://doi.org/10.1016/j.cbpa.2022.102155.

Kroezen, V., F. S. Schenkel, F. Miglior, C. F. Baes, and E. J. Squires. 2018. Candidate gene association analyses for ketosis resistance in Holsteins. J. Dairy Sci. 101:5240–5249. https://doi.org/10.3168/jds.2017-13374.

Lavery, A., and C. P. Ferris. 2021. Proxy measures and novel strategies for estimating nitrogen utilisation efficiency in dairy cattle. Animals (Basel) 11:343. https://doi.org/10.3390/ani11020343.

Lee, J., K. Cho, K. A. Weigel, H. M. White, C. Do, and I. Choi. 2024. Identification of genomic regions and genes associated with subclinical ketosis in periparturient dairy cows. J. Anim. Sci. Technol. 66:567–576. https://doi.org/10.5187/jast.2023.e97.

Lee, S., K. Cho, M. Park, T. Choi, S. Kim, and C. Do. 2016. Genetic parameters of milk β-hydroxybutyric acid and acetone and their genetic association with milk production traits of Holstein cattle. Asian-Australas. J. Anim. Sci. 29:1530–1540. https://doi.org/10.5713/ajas.16.0310.

Magro, S., A. Costa, D. Cavallini, E. Chiarin, and M. De Marchi. 2024. Phenotypic variation of dairy cows' hematic metabolites and feasibility of non-invasive monitoring of the metabolic status in the transition period. Front. Vet. Sci. 11:1437352. https://doi.org/10.3389/fvets.2024.1437352.

Magro, S., M. De Marchi, M. Cassandro, R. Finocchiaro, A. Fabris, M. Marusi, and A. Costa. 2025. Blood parameters predicted from milk spectra are candidate indicator traits of hyperketonemia—A retrospective study in the Italian Holstein population. J. Dairy Sci. 108:2683–2696. https://doi.org/10.3168/jds.2024-25170.

Matenchi, Y. P., E. K. Bastanlar, and M. Hegarty. 2025. Genome-wide association analysis revealed novel candidate genes for body measurement traits in indigenous Gudali and crossbred Simgud in Cameroon. BMC Genomics 26:664. https://doi.org/10.1186/s12864-025-11865-7.

McArt, J. A. A., D. V. Nydam, and G. R. Oetzel. 2012. Epidemiology of subclinical ketosis in early lactation dairy cattle. J. Dairy Sci. 95:5056–5066. https://doi.org/10.3168/jds.2012-5443.

McCarthy, S. D., S. M. Waters, D. A. Kenny, M. G. Diskin, R. Fitzpatrick, J. Patton, D. C. Wathes, and D. G. Morris. 2010. Negative energy balance and hepatic gene expression patterns in high-yielding dairy cows during the early postpartum period: A global approach. Physiol. Genomics 42A:188–199. https://doi.org/10.1152/physiolgenomics.00118.2010.

Nayeri, S., F. Schenkel, A. Fleming, V. Kroezen, M. Sargolzaei, C. Baes, A. Cánovas, J. Squires, and F. Miglior. 2019. Genome-wide association analysis for β-hydroxybutyrate concentration in milk in Holstein dairy cattle. BMC Genet. 20:58. https://doi.org/10.1186/s12863-019-0761-9.

Ning, M., Y. Zhao, D. Dai, C. Yao, H. Liu, L. Fang, B. Wang, Y. Zhang, and J. Cao. 2023. Gene co-expression network and differential expression analyses of subcutaneous white adipose tissue reveal novel insights into the pathological mechanisms underlying ketosis in dairy cows. J. Dairy Sci. 106:5018–5028. https://doi.org/10.3168/jds.2022-22941.

Oliveira-Junior, G. A., F. S. Schenkel, L. Alcantra, K. Houlahan, C. Lynch, and C. F. Baes. 2021. Estimated genetic parameters for all genetically evaluated traits in Canadian Holsteins. J. Dairy Sci. 104:9002–9015. https://doi.org/10.3168/jds.2021-20227.

Ospina, P. A., D. Nydam, T. Stokol, and T. Overton. 2010. Associations of elevated nonesterified fatty acids and [beta]-hydroxybutyrate concentrations with early lactation reproductive performance and milk production in transition dairy cattle in the northeastern United States. J. Dairy Sci. 93:1596–1603. https://doi.org/10.3168/jds.2009-2852.

Pryce, J. E., K. L. Parker Gaddis, A. Koeck, C. Bastin, M. Abdelsayed, N. Gengler, F. Miglior, B. Heringstad, C. Egger-Danner, K. F. Stock, A. J. Bradley, and J. B. Cole. 2016. Invited review: Opportunities for genetic improvement of metabolic diseases. J. Dairy Sci. 99:6855–6873. https://doi.org/10.3168/jds.2016-10854.

Raboisson, D., M. Mounié, and E. Maigné. 2014. Diseases, reproductive performance, and changes in milk production associated with subclinical ketosis in dairy cows: A meta-analysis and review. J. Dairy Sci. 97:7547–7563. https://doi.org/10.3168/jds.2014-8237.

Rasmussen, P., H. W. Barkema, P. P. Osei, J. Taylor, A. P. Shaw, B. Conrady, G. Chaters, V. Muñoz, D. C. Hall, O. O. Apenteng, J. Rushton, and P. R. Torgerson. 2024. Global losses due to dairy cattle diseases: A comorbidity-adjusted economic analysis. J. Dairy Sci. 107:6945–6970. https://doi.org/10.3168/jds.2023-24626.

Rico, J. E., and M. A. Barrientos-Blanco. 2024. Invited review: Ketone biology—The shifting paradigm of ketones and ketosis in the dairy cow. J. Dairy Sci. 107:3367–3388. https://doi.org/10.3168/jds.2023-23904.

Sadri, H., M. H. Ghaffari, and H. Sauerwein. 2023. Invited review: Muscle protein breakdown and its assessment in periparturient dairy cows. J. Dairy Sci. 106:822–842. https://doi.org/10.3168/jds.2022-22068.

Sahana, G., Z. Cai, M. P. Sanchez, A. C. Bouwman, and D. Boichard. 2023. Invited review: Good practices in genome-wide association studies to identify candidate sequence variants in dairy cattle. J. Dairy Sci. 106:5218–5241. https://doi.org/10.3168/jds.2022-22694.

Schmidtke, C., S. Tiede, M. Thelen, R. Käkelä, S. Jabs, G. Makrypidi, M. Sylvester, I. Schweizer, M. Braren, N. Brocke-Ahmadinejad, S. L. Cotman, A. Schulz, V. Gieselmann, and T. Braulke. 2019. Lysosomal proteome analysis reveals that CLN3-defective cells have multiple enzyme deficiencies associated with changes in intracellular trafficking. J. Biol. Chem. 294:9592–9604. https://doi.org/10.1074/jbc.RA119.008852.

Seely, C. R., K. D. Bach, D. M. Barbano, and J. A. A. McArt. 2021. Effect of hyperketonemia on the diurnal patterns of energy-related blood metabolites in early-lactation dairy cows. J. Dairy Sci. 104:818–825. https://doi.org/10.3168/jds.2020-18930.

Steeneveld, W., P. Amuta, F. J. van Soest, R. Jorritsma, and H. Hogeveen. 2020. Estimating the combined costs of clinical and subclinical ketosis in dairy cows. PLoS One 15:0230448. https://doi.org/10.1371/journal.pone.0230448.

Surma, M. A., C. Klose, and K. Simons. 2012. Lipid-dependent protein sorting at the trans-Golgi network. Biochim. Biophys. Acta Mol. Cell Biol. Lipids 1821:1059–1067. https://doi.org/10.1016/j.bbalip.2011.12.008.

Suthar, V. S., J. Canelas-Raposo, A. Deniz, and W. Heuwieser. 2013. Prevalence of subclinical ketosis and relationships with postpartum diseases in European dairy cows. J. Dairy Sci. 96:2925–2938. https://doi.org/10.3168/jds.2012-6035.

Trevisi, E., and A. Minuti. 2018. Assessment of the innate immune response in the periparturient cow. Res. Vet. Sci. 116:47–54. https://doi.org/10.1016/j.rvsc.2017.12.001.

van den Berg, I., P. N. Ho, T. V. Nguyen, M. Haile-Mariam, T. D. Luke, and J. E. Pryce. 2022. Using mid-infrared spectroscopy to increase GWAS power to detect QTL associated with blood urea nitrogen. Genet. Sel. Evol. 54:27. https://doi.org/10.1186/s12711-022-00719-5.

von Blume, J., and A. Hausser. 2019. Lipid-dependent coupling of secretory cargo sorting and trafficking at the trans-Golgi network. FEBS Lett. 593:2412–2427. https://doi.org/10.1002/1873-3468.13552.

Wathes, D. C., F. Becker, L. Buggiotti, M. A. Crowe, C. Ferris, L. Foldager, C. Grelet, M. Hostens, K. L. Ingvartsen, C. Marchitelli, M. Salavati, F. Signorelli, H. Takeda, L. Tang, and Z. Cheng. 2021. Associations between circulating IGF-1 concentrations, disease status and the leukocyte transcriptome in early lactation dairy cows. Ruminants 1:147–177. https://doi.org/10.3390/ruminants1020012.

Wathes, D. C., Z. Cheng, W. Chowdhury, M. A. Fenwick, R. Fitzpatrick, D. G. Morris, J. Patton, and J. J. Murphy. 2009. Negative energy balance alters global gene expression and immune responses in the uterus of postpartum dairy cows. Physiol. Genomics 39:1–13. https://doi.org/10.1152/physiolgenomics.00064.2009.

Xu, Q., Y. Fan, J. J. Loor, Q. Jiang, X. Zheng, Z. Wang, T. Yang, X. Sun, H. Jia, X. Li, and C. Xu. 2022. Effects of diacylglycerol O-acyltransferase 1 (DGAT1) on endoplasmic reticulum stress and inflammatory responses in adipose tissue of ketotic dairy cows. J. Dairy Sci. 105:9191–9205. https://doi.org/10.3168/jds.2022-21989.

Yang, J., S. H. Lee, M. E. Goddard, and P. M. Visscher. 2011. GCTA: A tool for genome-wide complex trait analysis. Am. J. Hum. Genet. 88:76–82. https://doi.org/10.1016/j.ajhg.2010.11.011.

Yin, L. 2016. User manual for CMPLOT—Circular Manhattan plot. Accessed May 12, 2025. https://cran.r-project.org/web/packages/CMplot/CMplot.pdf.

Zhang, G., D. Hailemariam, E. Dervishi, S. A. Goldansaz, Q. Deng, S. M. Dunn, and B. N. Ametaj. 2016. Dairy cows affected by ketosis show alterations in innate immunity and lipid and carbohydrate metabolism during the dry off period and postpartum. Res. Vet. Sci. 107:246–256. https://doi.org/10.1016/j.rvsc.2016.06.012.

Zou, Y., N. Gong, Y. Cui, X. Wang, A. Cui, Q. I. Chen, T. Jiao, X. Dong, H. Yang, S. Zhang, F. Fang, and Y. Chang. 2015. Forkhead box P1 (FOXP1) transcription factor regulates hepatic glucose homeostasis. J. Biol. Chem. 290:30607–30615. https://doi.org/10.1074/jbc.M115.681627.

ORCIDS

S. Magro, https://orcid.org/0000-0001-6257-5158
A. Costa, https://orcid.org/0000-0001-5353-8988
J. B. C. H. M. van Kaam, https://orcid.org/0000-0002-2592-2461
R. Finocchiaro, https://orcid.org/0000-0002-9058-9992
M. Cassandro, https://orcid.org/0000-0002-8709-2870
M. De Marchi https://orcid.org/0000-0001-7814-2525